Tang Ba Dai, 2026, 14:1
ISSN (Online): 2348-4098
ISSN (Print): 2395-4752

International Journal of Science, Engineering and Technology
An Open Access Journal

Effect of SiO_2, MnO_2, and TiO_2 Contents on the Tensile Strength of Butt Welded Joints in Low-Alloy Steel

Tang Ba Dai
Viet Hung Industrial University, Hanoi, Vietnam

Abstract- This paper presents a method for predicting the tensile strength of Q460 low-alloy steel welds produced by submerged arc welding using ceramic flux, based on experimental data and analysis of variance (ANOVA). The selection of appropriate welding parameters, electrode wire, and ceramic flux composition compatible with the base metal is evaluated through mechanical testing to determine the strength and reliability of the welded structure, thereby enabling adjustments to flux composition or welding parameters if necessary. In this study, the ceramic flux mixture consists of SiO_2, MnO_2, and TiO_2 as the main components, combined at different percentage ratios. The experiments were designed using the Taguchi L9 method and analyzed using ANOVA. The analysis shows that the percentage contributions to tensile strength are as follows: SiO_2 = 24.13%, MnO_2 = 12.78%, and TiO_2 = 63.69%.

Keywords: Optimization, Submerged Arc Welding (SAW), Taguchi Method, ANOVA.

I. INTRODUCTION

Submerged arc welding (SAW) using ceramic flux is widely adopted in heavy industry and structural engineering, particularly in shipbuilding, large-diameter pipe welding, and heavy-duty structures. A weld joint is considered durable if it is free from hydrogen-induced cracking, gas porosity, slag inclusions, and other defects. In SAW, weld quality is critically determined by the choice of wire diameter, flux composition, and welding parameters. Research confirms that welding parameters, ceramic flux composition, and the selection of welding wire suitable for the base metal are key factors influencing weld strength [1].

Important characteristics, such as improved slag detachability, arc stability, and weld alloying, are known to increase with higher SiO_2 content in the flux composition [2]. The presence of manganese (Mn) and calcium silicate ($CaSiO_3$) effectively reduces sulfur levels and removes phosphorus from the weld pool [3]. However, high contents of SiO_2 and TiO_2 increase heat input but can adversely affect the mechanical properties of the weld [4]. In SAW, arc voltage is particularly important when using SiO_2-based fluxes [5]. The formation of acicular ferrite (AF) in the weld structure, controlled by oxides such as CaO, contributes significantly to desirable mechanical properties like toughness and impact strength [6].

The combined effect of the welding wire and the chemical composition of the flux influences the transformation of slag and weld metal, which has been shown to improve tensile strength and load-bearing capacity of the weld metal [7]. FeO content in the slag governs oxygen levels during welding; although low oxygen content is required in the weld metal, the decomposition of SiO_2 during welding must be taken into account. A detailed study compared the chemical composition of various flux batches alongside resulting weld structure and tensile strength in submerged arc welding [8].

The effects of chemical components in ceramic flux during SAW have been clearly explained through various experimental studies [9]. Ceramic welding flux plays a vital role in determining weld metal quality, which has been thoroughly elucidated by multiple testing methods [10]. Adjustments in MnO and Fe-Cr contents in the ceramic flux aim to achieve desired hardness limits in the weld metal [11]. Moreover, increasing MnO, MgO, and Fe-Cr content enhances the ductility of the weld metal [12]. Finally, the grain size of ceramic flux, typically ranging between 0.5 and 1.2 mm, and weld penetration depth can be optimized by adjusting the SiO_2 flux

composition and applying Taguchi analysis in SAW [13].

II. ANALYTICAL METHOD

Table 1. Tensile test results of Q460 steel specimens according to TCVN 197:2002

No.	Code	TiO2 (%)	SiO2 (%)	MnO2 (%)	Q460 Steel
					Tensile Strength (MPa)
1	0	8	12	18	587,0
2	11	8	14	20	454,0
3	22	8	16	22	564,0
4	101	10	12	20	669,0
5	112	10	14	22	566,0
6	120	10	16	18	674,0
7	202	12	12	22	634,0
8	210	12	14	18	671,0
9	221	12	16	20	680,0

Based on the experimental dataset (Table 1), analysis of variance (ANOVA) is employed to evaluate the influence of TiO_2, SiO_2, and MnO_2 proportions in the ceramic flux composition on the mechanical properties of the weld metal. This serves as the foundation for determining the optimal combination of these components to ensure the desired mechanical performance of the welded joint.

ANOVA is a statistical technique used when comparing the means of three or more groups. It allows quantification of the relative influence and significance of contributing factors on the target response. Since variance represents the degree of dispersion of observations relative to the mean, ANOVA facilitates the comparison of means by examining differences in variances among groups.

The steps in the analysis of variance (ANOVA) include:
Step 1: Assign factor levels.
Step 2: Calculate the sum of experimental results.
Step 3: Compute the correction factor for the factors.
Step 4: Calculate the sum of squares for each factor.
Step 5: Determine the degrees of freedom for the experiment and for each factor.
Step 6: Calculate the mean squares (variance) of the factors.
Step 7: Calculate the total sum of squares as the basis for comparing the variation around the mean.
Step 8: Calculate the percentage contribution of each factor to the objective function.
Step 9: Compile the results into the ANOVA table.

III. RESULTS AND DISCUSSION

Based on the content and implementation steps of the Taguchi method, the influence analysis and determination of the optimal proportion of flux components to ensure the weld joint strength were conducted as follows:

Step 1: The selected objective function is the tensile strength (σ_b) of the weld joint. The factors influencing this objective function include TiO_2, SiO_2, and MnO_2.
Step 2: Each influencing factor was assigned three levels with specific values, as shown in Table 2.

Table 2. Levels and corresponding values of influencing factors

Factor	Level 1 (%)	Level 2 (%)	Level 3 (%)
TiO_2	8	10	12
SiO_2	12	14	16
MnO_2	18	20	22

With three factors each at three levels, the L9 orthogonal array was selected. Accordingly, nine experimental conditions were established, corresponding to the nine rows in Table 3.

Table 3. Experimental conditions, measured results, and S/N ratios of tensile strength

No.	M	TiO_2 (%)	SiO_2 (%)	MnO_2 (%)	σb (MPa)	y_i^2	MSD (10-6)	S/N
1	0	8	12	18	587	344569	2.90	55.37
2	11	8	14	20	454	206116	4.85	53.14
3	22	8	16	22	564	318096	3.14	55.03
4	101	10	12	20	669	447561	2.23	56.51
5	112	10	14	22	566	320356	3.12	55.06

6	120	10	16	18	674	454276	2.20	56.57
7	202	12	12	22	634	401956	2.49	56.04
8	210	12	14	18	671	450241	2.22	56.53
9	221	12	16	20	680	462400	2.16	56.65

Step 3: The experiments were conducted according to the conditions listed above, and the tensile strength values corresponding to each experimental condition were recorded. The measured tensile strength values are presented in Column 6 of Table 3.

Step 4: The S/N ratio was calculated based on the "larger-the-better" quality characteristic. The resulting S/N ratios for each experimental condition are shown in Column 9 of Table 3.

To quantitatively evaluate the influence of TiO_2, SiO_2, and MnO_2 on the tensile strength of the weld joint and to determine the optimal factor levels, an ANOVA analysis was performed. Based on the S/N ratio results in Table 3, the ANOVA parameters were computed. The results are summarized in Table 4.

Table 4. Factor levels and percentage contributions of factors to weld tensile strength

Experiment	1	2	3	4	5	6	7	8	9
σb (MPa)	587	454	564	669	566	674	634	671	680

Mean tensile strength, m (MPa)		611
Total of experimental results, T		5499
Correction factor, CF		3359889
Total degrees of freedom, fT		8
Leveling of parameters (mji)	$m(TiO_2)_1$	54,51
	$m(TiO_2)_2$	56,05
	$m(TiO_2)_3$	56,41
	$m(SiO_2)_1$	55,97
	$m(SiO_2)_2$	54,91
	$m(SiO_2)_3$	56,08
	$m(MnO_2)_1$	55,97
	$m(MnO_2)$	54,91
	$m(MnO_2)$	56,08
Sum of Squares (Sj)	STiO2	56,16
	SSiO2	55,43
	SMnO2	55,37
Total sum of squares (ST)	42321,33	
Degrees of Freedom (fj)	fTiO2	2
	fSiO2	2
	fMnO2	2
Mean Square Values (Vj)	VTiO2	13477,33
	VSiO2	5106,33
	VMnO2	2577
Percentage Contribution (Pj)	PTiO2	63,69
	PSiO2	24,13
	PMnO2	12,18

Based on the experimental results (Table 3) and the ANOVA procedure, the factor-level plots and percentage contribution charts were constructed, as shown in Figures 1 and 2. Note that X, Y, and Z correspond to TiO_2, SiO_2, and MnO_2, respectively.

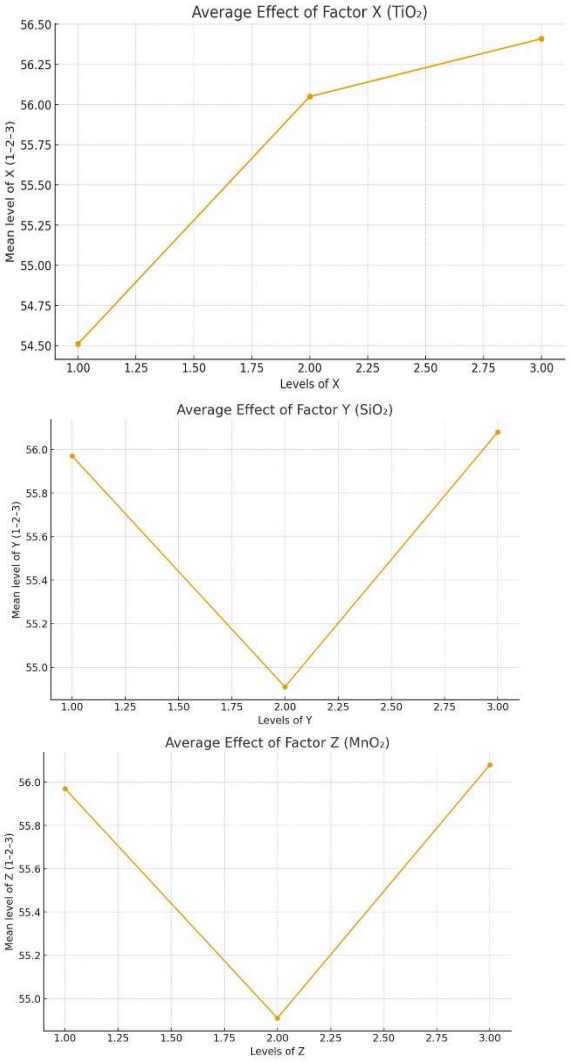

Figure 1. Level plots of the factors for the tensile strength of the weld joint
a) Level plot of TiO_2; b) Level plot of SiO_2; c) Level plot of MnO_2

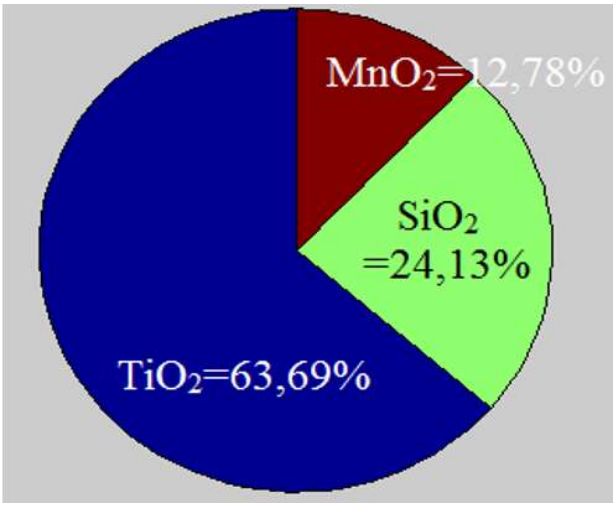

Figure 2. Percentage contribution of the factors TiO_2, SiO_2, and MnO_2 to the tensile strength of the weld joint

Based on the level plots of the factors, it can be observed that:

For the "larger-the-better" quality characteristic, the optimal levels of the factors to achieve the maximum tensile strength are TiO_2 at level 3, SiO_2 at level 3, and MnO_2 at level 1. The predicted tensile strength corresponding to the combination of factors at these optimal levels obtained from the experiment is:

$$Y_{opt} = T + (X_3 - T) + (Y_3 - T) + (Z_1 - T) = 723\ (Mpa)$$

The regression model is established in the form of a multiplicative function as follows:

$$\sigma_b = b_0 X^{b_1} Y^{b_2} Z^{b_3} \quad (1)$$

Taking the logarithm (base 2) of both sides of equation (1), we obtain:

$$\ln \sigma_b = \ln b_0 + b_1 \ln X + b_2 \ln Y + b_3 \ln Z \quad (2)$$

Let:

$$\tilde{\sigma}_b = \ln \sigma_b;\ \ a_0 = \ln b_0;\ \ a_1 = b_1; a_2 = b_2;\ a_3 = b_3; x = \ln(X); y = \ln(Y); z = \ln(Z) \quad (3)$$

$$\tilde{\sigma}_b = a_0 + a_1 x + a_2 y + a_3 z \quad (4)$$

Here, the coefficients a0, a1, a2, a3 are unknown and need to be determined.

Meanwhile, x, y, z are the logarithms of the corresponding factor levels TiO_2, SiO_2, MnO_2 in the experiment.

Using the least squares method, the objective is to determine the coefficients a0, a1, a2, a3 such that the following expression is minimized:

$$S(a_0, a_1, a_2, a_3) = \sum_{i=1}^{n} \left[(\sigma_b)_i - \tilde{\sigma}_b(x_i, y_i, z_i) \right]^2 \to \min$$

or equivalently:

$$S(a_0, a_1, a_2, a_3) =$$

$$= \sum_{i=1}^{n} \left[(\sigma_b)_i - (a_0 + a_1.x_i + a_2.y_i + a_3.z_i) \right]^2 \to \min$$

In these expressions, $(\sigma_b)_i$ represents the experimentally measured values, whereas $\tilde{\sigma}_b$ denotes the corresponding theoretical values predicted by the regression model. The necessary conditions for minimizing the objective function are obtained from:

$$\frac{\partial S}{\partial a_j} = \sum_{i=1}^{9} \left[(\sigma_b)_i - \tilde{\sigma}_b(x_i, y_i, z_i) \right]^2 = 0 \quad (j = 1...3)$$

Thus:

$$\begin{cases} \dfrac{\partial S}{\partial a_0} = \sum_{i=1}^{9} (2a_1 x_i + 2a_3 z_i + 2a_2 y_i + 2a_0 - 2\sigma_i) = 0 \\ \dfrac{\partial S}{\partial a_1} = \sum_{i=1}^{9} 2x_i (a_1 x_i + a_3 z_i + a_2 y_i + a_0 - \sigma_i) = 0 \\ \dfrac{\partial S}{\partial a_2} = \sum_{i=1}^{9} 2y_i (a_1 x_i + a_3 z_i + a_2 y_i + a_0 - \sigma_i) = 0 \\ \dfrac{\partial S}{\partial a_3} = \sum_{i=1}^{9} 2z_i (a_1 x_i + a_3 z_i + a_2 y_i + a_0 - \sigma_i) = 0 \end{cases} \quad (5)$$

Solving the system of four linear equations (5) using an iterative algorithm implemented in MATLAB yields the following results:

$$\begin{cases} b_0 = 640,92; \\ b_1 = 0,547; \\ b_2 = 0,022; \\ b_3 = -0,457; \end{cases}$$

With the coefficients obtained above, the linear regression equation can be expressed as follows:

$$\sigma_b = 640,92 X^{0,547} Y^{0,022} Z^{-0,457} \quad (6)$$

As previously determined, the optimal levels for achieving the highest tensile strength are: TiO_2 at level 3, SiO_2 at level 3, and MnO_2 at level 1.

Combining these optimal factor levels with the regression equation (6), the influence of the flux

component proportions on tensile strength is illustrated in the following plots.

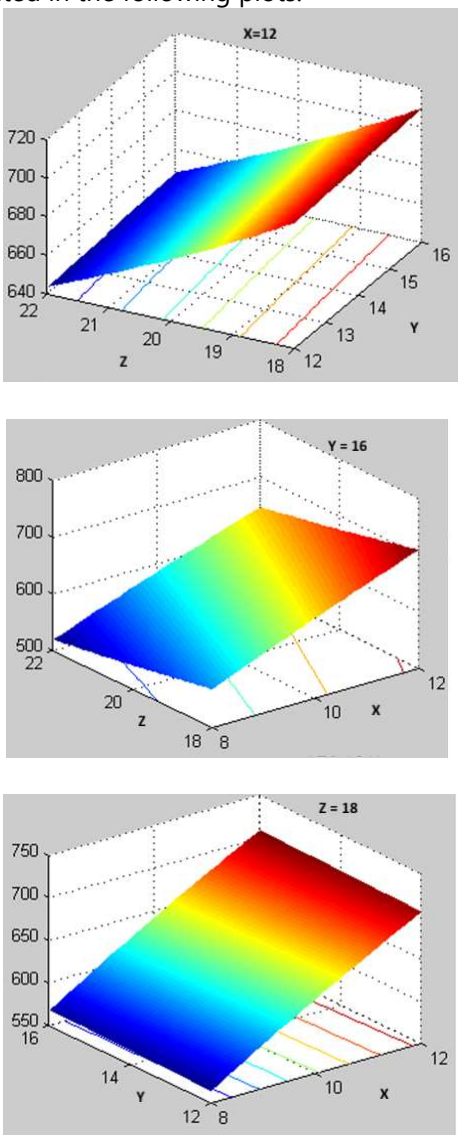

Figure 3. 3D power-law surface plots showing the dependence of tensile strength on individual flux components at their optimal levels

Based on the plots describing the dependence of tensile strength on the proportions of the flux components and regression equation (6), the following observations can be made:

The tensile strength of the weld joint is directly proportional to TiO_2 and SiO_2, and inversely proportional to MnO_2.

From Figure 3a, an increase in SiO_2 leads to an increase in tensile strength. Conversely, increasing MnO_2 results in a decrease in tensile strength.
Similarly, increasing TiO_2 increases the tensile strength, while increasing MnO_2 decreases it (Figure 3b).

The tensile strength increases significantly when both TiO_2 and SiO_2 are increased simultaneously (Figure 3c).

IV. CONCLUSION

Based on the experimental results, analysis, and evaluation of nine weld samples prepared with nine different batches of filler mixtures, several conclusions can be drawn.

From the distribution graph illustrating the influence of TiO_2, SiO_2, and MnO_2 on the tensile strength of the welds, it was observed that TiO_2 has the most significant effect at 63.69%, followed by SiO_2 with a moderate effect of 24.13%, and MnO_2 with the least effect at 12.78%. This distribution indicates that, when designing welds to achieve high tensile strength, priority should be given to adjusting the proportion of TiO_2.

Therefore, the tensile strength of the welds depends on the ratios of TiO_2, SiO_2, and MnO_2 in the ceramic welding flux. To establish a mathematical relationship between these components and the target variable, i.e., the tensile strength of the welds, and to analyze the trend of their influence as well as assess the effect of technological parameters on the target variable, the least squares method was employed to construct a mathematical model. This model represents the dependence of weld tensile strength on the proportions of TiO_2, SiO_2, and MnO_2 in the ceramic flux.

Acknowledgements
The author sincerely thanks the faculty and technical staff at Viet-Hung Industrial University for their invaluable support throughout the experimental work. Special appreciation is extended to the laboratory team for their assistance in conducting welding tests and mechanical measurements. The

author also gratefully acknowledges the constructive feedback provided by colleagues and reviewers.

REFERENCES

1. N. M. R. De Rissone, J. P. Faris, I. De Souza Bott, "ANSI/AWS A5.1-91 E6013 Rutile Electrodes: The Effect of Calcite," AWS, pp. 113S–123S, 2002.
2. U. Masao, Z. Bahaa, M. Wafaa, Adbe-Monen, "Effect of Arc Welding Flux Chemical Composition on Weldment Performance," Trans JWRI, Vol. 24, No. 1, pp. 45–53, 1995.
3. U. Mitra, T. W. Eagar, "Slag Metal Reaction During Submerged Arc Welding of Alloy Steels," Metall Trans, pp. 217–226, 1984.
4. K. Prasad, D. K. Dwivedi, "Microstructure and Tensile Properties of Submerged Arc Welded 1.25 Cr-0.5Mo Steel Joint," Materials and Manufacturing Processes, Vol. 23, pp. 463–468, 2008.
5. C. Yang, S. Lin, F. Liu, L. Wu, "Research on the Mechanism of Penetration Increase by Flux in A-TIG Welding," J Mater Sci Techno, Vol. 19, No. 1, pp. 225–227, 2003.
6. P. Kanjilal, S. K. Majumdar, T. K. Pal, "Prediction of Acicular Ferrite From Flux Ingredients in Submerged Arc Weld Metal of C-Mn Steel," ISIJ International, Vol. 45, No. 6, pp. 876–885, 2005.
7. B. Kook-Soo, P. Chan, J. Hong-Chul, "Effect of Flux Composition on the Element Transfer and Mechanical Properties of Weld Metal in Submerged Arc Welding," Met Mater Int, Vol. 15, No. 3, pp. 471–477, 2009.
8. T. W. Eagar, "Source of Weld Metal Oxygen Contamination During Submerged Arc Welding," Welding Journal Research Supplement, 1978.
9. L. I. Qing-Ming, W. Hong, Z. Da Zeng, "Effect of Activating Flux on Arc Shape and Arc Voltage in Tungsten Gas Welding," Transaction of Nonferrous Metals Society of China, Vol. 17, pp. 486–490, 2007.
10. M. Paniagua Mercado, V. M. Lopez-Hirata, L. M. Munoz Saucedo, "Influence of the Chemical Composition of Flux on the Microstructure and Tensile Properties of Submerged-Arc Welds," Journal of Materials Processing Technology, Vol. 169, pp. 346–351, 2005.
11. K. Singh, S. Pandey, "Recycling of Slag to Act as a Flux in Submerged Arc Welding," Resources, Conservation and Recycling, Vol. 53, pp. 552–558, 2009.
12. Kumar, H. Singh, S. Maheshwari, "Modelling and Analysis by Response Surface Methodology of Hardness for Submerged Arc Welded Joints Using Developed Agglomerated Fluxes," Indian Journal of Engineering and Material Sciences, Vol. 19, pp. 379–385, 2012.
13. Kumar, S. Maheshwari, "Optimization of Weld Bead for Rutile Based Flux Constituents by Taguchi Analysis in Submerged Arc Welding," International Journal of Applied Engineering Research, Vol. 10, No. 78, pp. 95–98, 2015.
14. E. Kumari, B. Choudhary, "Hydrogen Is the Future of Energy Security and Sustainability: A Review," Journal of Mechanical and Construction Engineering (JMCE), Vol. 3, Iss. 2, S. No. 001, pp. 1–13, 2023.
15. G. M. Azanaw, "Application of Digital Twin in Structural Health Monitoring of Civil Structures: A Systematic Literature Review Based on PRISMA," Journal of Mechanical and Construction Engineering (JMCE), Vol. 4, Iss. 1, S. No. 001, pp. 1–10, 2024.